https://doi.org/10.5194/egusphere-2025-2886
Preprint. Discussion started: 7 July 2025

Icebergs, jigsaw puzzles and genealogy: Automated multi-generational iceberg tracking and lineage reconstruction.

Ben R. Evans[1], Alan R. Lowe[2], Anna Crawford[3], Andrew Fleming[1], J. Scott Hosking[1,2]

[1] British Antarctic Survey, Cambridge, CB3 0ET, UK
[2] Alan Turing Institute, London, NW1 2DB, UK
[3] University of Stirling, Stirling, FK9 4LA, UK

Correspondence to: Ben R. Evans (benevans@bas.ac.uk)

Abstract. Tabular icebergs calve from ice shelves and glaciers in Antarctica, Greenland, and northern Ellesmere Island. These 'ice islands', as they are referred to in the Arctic, drift, melt, and fragment, contributing freshwater and nutrients to the ocean, influencing circulation, carbon cycling and biodiversity in ways that remain poorly understood. Icebergs also pose risks to shipping, and maritime infrastructure. Improved understanding of iceberg drift and fragmentation will reduce uncertainties in climate simulations and operational hazards. This study presents the first comprehensively validated, scalable iceberg tracking approach and the first that is capable of reconstructing iceberg 'lineages' (here used to describe life histories including sources, where that source is a larger iceberg) through fragmentation events. This method enables a comprehensive reconstruction of iceberg paths from calving to their eventual disintegration, allowing for monitoring and source attribution across their life cycle.

We propose CryoTrack, an unsupervised approach based on iceberg geometry that is agnostic to data source or delineation method. The system requires only vector outlines. Initially, icebergs are linked across timesteps when their shapes remain similar, forming 'tracklets'. When significant shape changes occur, fragmented 'child' icebergs are linked to their 'parents' using a fuzzy geometric assembly method based on dynamic time warping, akin to assembling a jigsaw puzzle without image data. This approach reconstructs full iceberg lineages back to their calving origin. We evaluate system performance using manually tracked iceberg outlines originating from Petermann Glacier and other northwest Greenland ice tongues. Standard tracking metrics and custom iceberg specific metrics assess its accuracy in scientific and operational contexts. Our approach achieves excellent tracking of icebergs with an overall tracking accuracy of 0.98 and 94% of iceberg area are correctly linked to source when icebergs are last observed.

This system contributes to the need for scalable iceberg monitoring. It enhances understanding of iceberg behaviours, impacts, and fragmentation, supporting process based and data driven predictive modelling for environmental and operational applications.

1 Introduction

Freshwater inputs to the oceans due to iceberg melting have the potential to influence ocean circulations, sea ice formation and nutrient and carbon cycles, with global environmental repercussions, yet iceberg dynamics and impacts are poorly represented

https://doi.org/10.5194/egusphere-2025-2886
Preprint. Discussion started: 7 July 2025

in numerical models due to a paucity of observations (Cenedese & Straneo, 2023). Iceberg flux represents roughly half of the total freshwater discharge from both the Antarctic and Greenland ice sheets (Bamber et al., 2012; Bamber et al., 2018; Depoorter et al., 2013; Rignot et al., 2013). The locations of this freshwater input to the oceans can be far from the source location and substantially temporally delayed (Wagner et al., 2017), making this input difficult to quantify and model. For tabular Antarctic icebergs, 80% of ice loss has been shown to result from fragmentation into smaller icebergs, compared to 18% from basal melt (Tournadre et al., 2015). Being able to identify the source of large bergs and their fragments is therefore crucial to understanding the location and timing of most of the freshwater input to the oceans from icebergs. This capability would enable better parameterizations of freshwater distributions in ocean models (Huth et al., 2022; Marsh et al., 2015), improve their coupling to ice sheet models (Shiggins et al., 2023), aid evaluation of ecological impacts (Arrigo et al., 2002; K. L. Smith et al., 2013) and help mitigate hazards posed to humans, infrastructure and the environment (Fuglem & Jordaan, 2017; Hill, 2001; Mueller et al., 2013; Sackinger et al., 1985).

Icebergs are currently monitored by multiple national agencies for the provision of ice hazard information to marine stakeholders in the Arctic (e.g. Canadian Ice Service, International Ice Patrol), while the largest Antarctic icebergs (>18.5km in length) are tracked by the US National Ice Center. This tracking remains a largely manual endeavour. The requirement for substantial operator input limits current iceberg monitoring at both poles with restrictions to monitoring imposed based on geographical extents or iceberg size (e.g., Crawford et al., 2018a). Automated approaches to tracking will lead to more information being available to marine operators and will grow more extensive datasets for investigations into iceberg occurrence, drift and deterioration over time and space. As satellite technology improves, these automatically acquired datasets will also account for a greater proportion of the power law distribution that represents iceberg populations undergoing fragmentation (Crawford et al., 2018b; Enderlin et al., 2016; Tournadre et al., 2016). Such studies will furnish new insights to controls on motion (Crawford et al., 2016; Marson et al., 2018; Morison & Goldberg, 2012), fragmentation (A. J. Crawford et al., 2024; England et al., 2020; Huth, Adcroft, Sergienko, et al., 2022; Zeinali-Torbati et al., 2021) and freshwater inputs (Crawford et al., 2018b; Huth et al., 2022; Stern et al., 2016). These advances will, in turn, support improved modelling of ice-shelf fracture and calving by enabling more comprehensive evaluation and validation. Improved representation of the processes and drivers of iceberg drift and deterioration will also further efforts to integrate process based and data driven models across the ice sheet-ocean interface, enhancing the fidelity of global climate models (Ackermann et al., 2024; R. S. Smith et al., 2021).

Advances have been made in automatic iceberg identification from satellite imagery in recent years (Barbat et al., 2019; Moyer et al., 2019; Shiggins et al., 2023), though most approaches are not yet sufficiently scalable to support operational monitoring (Evans et al., 2023) and developments in this field are ongoing. While iceberg detection is a necessary step, our work focuses specifically on the downstream task of tracking icebergs once they have been detected in a time series of satellite images. Previously Barbat et al. (2021) developed an automated approach for tracking icebergs present in satellite scenes of the Weddell Sea. That approach relied on Jaccard similarity between shape descriptors, principally a vector of radial distances from centroid to perimeter. They used the tracked icebergs to infer drift and melt rates but did not attempt to link across fragmentation events.

https://doi.org/10.5194/egusphere-2025-2886
Preprint. Discussion started: 7 July 2025

Indeed, they observed that their tracker's principal failure mode was when fragmentation or large melt events occurred, although they did not offer a comprehensive evaluation of the tracker's characteristics. Koo et al. (2023) used similar shape descriptors to track icebergs detected by their algorithm but did not present a substantial evaluation. Earlier attempts at tracking have also been made (e.g., Silva & Bigg, 2005) but no studies have yet tried to reconstruct lineages starting from an iceberg's source location and spanning fragmentation events. The majority of smaller (yet often still tabular) icebergs are calved from larger icebergs rather than directly from ice shelves (Tournadre et al., 2016). Understanding the sources and fates of these fragments of larger icebergs is therefore a critical aspect of understanding freshwater fluxes and distributions. This study addresses some of the challenges to better understanding the impacts of icebergs on the global system by presenting the first comprehensively evaluated, automatable and scalable iceberg tracking methodology of which we are aware, and also the first iceberg tracking schema capable of maintaining lineage associations between icebergs across fragmentation events.

Tracking of icebergs sits within the broad domain of Multiple Object Tracking (MOT) problems. Most MOT methods are based on tracking unchanging objects in sequences of natural images and transformer architectures have recently been widely employed to produce state-of-the-art (SOTA) trackers (e.g., Chu et al., n.d.; Meinhardt et al., n.d.; Sun et al., 2020). The iceberg tracking problem is, perhaps, most similar to the problem of tracking cells in live cell microscopy data since both contexts must be able to handle division of objects (fragmentation for icebergs / mitosis in the context of cells), as well as movement, changes in shape and other attributes, and disappearance (melt / apoptosis). Cell tracking is a well developed field (Ulman et al., 2017) with transformer based architectures also recently achieving SOTA performance. Gallusser & Weigert (2025) recently proposed the first transformer tracking approach that is capable of handling division events. Nevertheless, and irrespective of architecture, we are not aware of any tracking approaches explicitly designed to be capable of handling division into more than two child objects, which is necessary for tracing the lineage of large tabular icebergs that may experience large fragmentation events that produce many child icebergs.

The iceberg tracking problem is further differentiated from other tracking challenges by the geospatial context, topological constraints, and complex environmental fields (wind, currents, sea ice concentration and drift etc.) that dictate iceberg movement. Additionally, the objects to be tracked vary dramatically in size. The surface area of tabular icebergs tracked in the the Canadian Ice Island Detection, Drift and Deterioration (CI2D3) Database, upon which we base this study, vary by 5 orders of magnitude (Crawford et al., 2018a). Their highly variable observed mobility, coupled with a sparse and irregular sampling frequency (relative to laboratory or video based sequence acquisitions available in microbiological studies) further exacerbates the tracking challenge for icebergs since they can move by hundreds of kilometres between observations to be well outside their previous footprint. There is also a pervasive missing data problem that arises from satellite acquisition schedules and meteorological conditions when constructing image sequences. Most MOT and cell tracking methods proposed to date are also supervised in nature and therefore require extensive datasets of manually labelled pairs of image and segmentation mask to learn object associations. While the CI2D3 Database (Crawford et al., 2018a) that we use to develop our presented approach contains numerous segmentations, the underlying image data are not available to the authors for the purposes of this study,

https://doi.org/10.5194/egusphere-2025-2886
Preprint. Discussion started: 7 July 2025

and we are not aware of any suitable annotated datasets upon which to train a supervised method. The approach proposed here is therefore fully unsupervised, which offers advantages for transferability across geographical contexts and data modalities. We employ tools and evaluation metrics developed for live cell tracking contexts but introduce a novel geometric assembly process along with evaluation metrics tailored to the expected downstream applications.

2 Data

We use the CI2D3 Database to develop and evaluate our proposed method. While other iceberg databases exist (e.g. Brigham-Young University / National Ice Center ((Budge & Long, 2018)), the CI2D3 Database is, to our knowledge, unique in containing comprehensive lineage information for icebergs down to, at times, 0.1km² in areal extent. The CI2D3 Database contains more than 25000 polygons, manually delineated from a combination RADARSAT-1 and -2 and Envisat imagery, representing large, tabular icebergs ("ice islands") that originated from calving events at the Petermann Glacier, northern Greenland in 2008, 2010, 2011 and 2012, along with calving events from other floating ice tongues in that region (Crawford et al., 2018a).

3 Methods

We adopt a tracking-by-detection approach to the problem, as is common across many MOT domains (Gallusser & Weigert, 2025). Within this framework, objects are initially segmented in a detection step before being tracked in a secondary step. In the case of manual delineations, as conducted for the generation of the CI2D3 Database, detections are in polygon (vector) format denoting the perimeter of the icebergs. Automated iceberg detection approaches vary but tend to produce segmentation masks representing presence or absence of iceberg on a per pixel basis. These can easily be converted to polygons. Some object detection methods may return properties of the identified regions (icebergs) such as texture or intensity, while others may return deep feature embeddings. However, these additional properties are not always available and would not be consistent across source data modalities. The tracker we propose here is therefore designed to operate on the lowest common denominator information supplied by all detection workflows, namely the geometry of each detection. This means it is highly generalizable and agnostic to the process that generates the iceberg segmentation. The tracking process consists of five stages: data preparation, tracklet construction, generational linking, lineage reconstruction and evaluation.

3.1 Data preparation

The contents of the CI2D3 Database are shown in Figure 1. We selected a spatial subset for development and evaluation that contains the calving tongue of the Petermann Glacier, the source of most of the icebergs in the dataset. The subset (delineated red in Figure 1) encompasses any icebergs from Petermann Glacier and those drifting from more northerly glaciers as they follow the prevalent drift pattern to the south through the Nares Strait. As such, the spatial extent of our subset encompasses the source of most icebergs and the densest field of observations in the dataset and should present the most challenging

https://doi.org/10.5194/egusphere-2025-2886
Preprint. Discussion started: 7 July 2025

environment in which to track icebergs because it contains the largest numbers of spatially close and contemporaneously observed icebergs, as well as the largest numbers of the smallest icebergs.

https://doi.org/10.5194/egusphere-2025-2886
Preprint. Discussion started: 7 July 2025

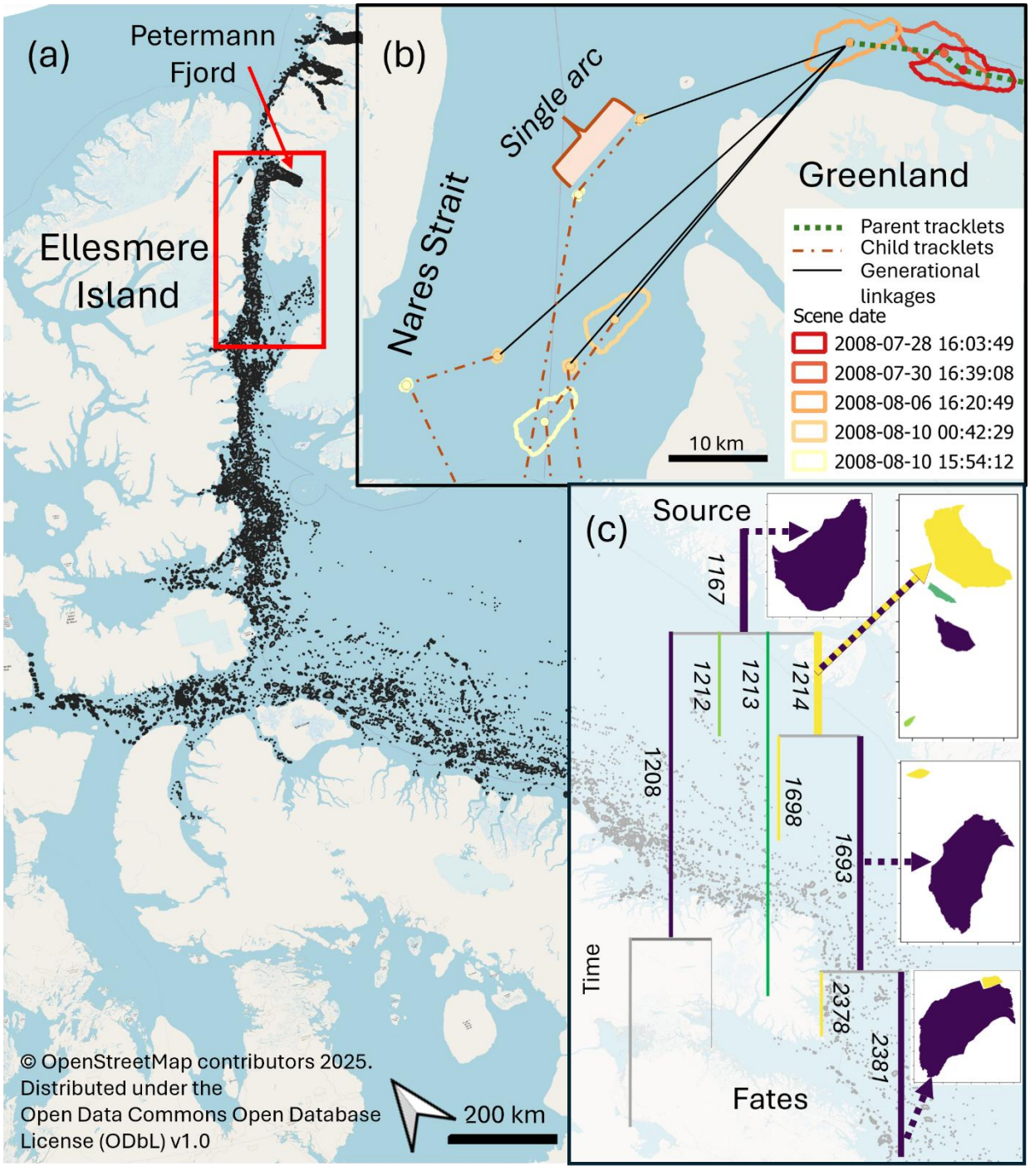

Figure 1: (a) Detections (black) in the CI2D3 Database spanning 2008-2013 with the spatial subset used here defined by the red box. (b) Example of tracklets and generational linkages for part of an iceberg lineage. (c) Schematic of partial lineage tree representing the fragmentation of an iceberg within the CI2D3 Database. Colours of branches correspond to the iceberg outlines on the right, numbers denote iceberg ID. Map data: https://www.openstreetmap.org/copyright.

https://doi.org/10.5194/egusphere-2025-2886
Preprint. Discussion started: 7 July 2025

Within the CI2D3 Database, each iceberg observation has a unique identifier, with lineage information contained in a field denoting, in the case of drift, the identifier associated with the previous observation of that iceberg or, in the case of fragmentation, the identifier will be that of the parent iceberg prior to fracture. This representation was initially converted for this study such that an iceberg retains the same unique (integer) identity across time points unless it divides into two or more fragments, at which point each child iceberg is assigned a new unique identifier and a 'parent' attribute denoting the ID of the iceberg that fragmented to form it ((c), Figure 1).

The domain contains multiple satellite scene footprints. Each observation timepoint, therefore, does not provide full coverage of the entire domain (even for the subset used in this study) and the remainder is effectively missing data. As such, the absence of icebergs in the missing data region does not imply an absence of icebergs at that point in time, merely an absence of observations. For any given location, therefore, the observations are temporally sparse relative to the overall sequence of all observation timepoints that comprise the whole domain. The target observation interval for any given point in the CI2D3 Database was two weeks. For the purposes of demonstrating the proposed method, the dates at which any observation was contained in the database were stacked and a uniformly incrementing timestep assigned to that date. For the test subset area this resulted in 706 observation timepoints between 2008 and 2013. We recognize that this simplistic treatment of the time domain presents issues but the development of a more general schema for simultaneously handling spatial and temporal sparsity within tracking problems is beyond the scope of the current work. Each polygon in the CI2D3 Database is represented by its geometry, which we resampled to a uniform 256 vertices, and has attributes of its own identity ('ID'), its parent's identity ('parent') and the timestep ('t') in which it was observed. In addition to these, the original iceberg to which each can track its lineage through its parents is denoted by a 'root' attribute.

3.2 Tracklet construction

The tracklet construction stage is analogous to the tracking approaches described in previous studies (Barbat et al., 2021; Koo et al., 2023; Silva & Bigg, 2005). In this stage, icebergs that do not change shape substantially between observations are linked, as illustrated by the dashed lines in panel B of Figure 1, where a tracklet refers to the path of a single iceberg, potentially across multiple consecutive observations. A path covering a single time step within a tracklet or generational linkage is referred to as an arc. The method must be able to associate icebergs that change slightly through time as they melt and small parts (below the detection limit) calve. We take a conceptually similar approach to that proposed by Barbat et al. (2021) in that we build associations between icebergs based on their size and shape. We derive five features to describe each shape. We use three simple features, namely area, length and perimeter. We use an additional two features to describe the complex geometry of the icebergs (UMAP-1 and UMAP-2). To compute these, we fit 10^{th} order elliptical fourier descriptors (EFDs, Kuhl & Giardina, 1982) to the perimeter shape, implemented using the pyefd python package (https://github.com/hbldh/pyefd, 2024). This results in 40 coeficients that are normalized to be rotation and translation invariant, but not size invariant. We then use a UMAP

https://doi.org/10.5194/egusphere-2025-2886
Preprint. Discussion started: 7 July 2025

dimensionality reduction (McInnes et al., 2018) to reduce this to the two additional features. All five features are rescaled 0-1. We then use Bayesian Tracker (Btrack, Ulicna et al. (2021)), a python package developed for live cell tracking, to establish tracklets for which geometric characteristics do not change dramatically. We use the 'visual features' linking but disable the motion model that places spatial priors on future iceberg locations since it is poorly suited to predicting the highly variable movement of icebergs and the non-uniform time spacing of observations. We also do not conduct global optimization, the step in which Btrack attempts to construct links between tracklets and establish parent-child relations since the heuristics are not appropriate for the iceberg context (see introduction). In the process of tracklet generation, Btrack computes a cosine distance between the feature vectors for all pairs of icebergs within a given search radius of each other before maximizing the likelihood of associations across the domain. Using the five visual features, the median cosine distance between icebergs and other temporal instances of the same identity was $3.2E^{-9}$, whereas the median distance to the icebergs with a different identity was seven orders of magnitude larger at 0.05. This indicates effective separation of geometries in this 5-dimensional feature space. To handle the temporal data sparsity problem arising from the large domain and intermittent satellite coverage of any one location within it, btrack is able to insert dummy instances for a prescribed number of timesteps between linked observations. If an iceberg is not observed again within the given time buffer the tracklet is terminated. The search radius and time buffer are tunable parameters that were set, through experimentation, at 100km and 6 timesteps respectively. Optimal values of these will be a function of the domain extent, data frequency and environmental factors controlling iceberg motion. Increasing them will tend to increase the false positive linkage rate while decreasing them will tend to increase the false negative rate.

3.3 Generational linking

Generational linking matches 'child' fragments to their 'parent', which is a larger iceberg, as shown as solid black lines in (b) of Figure 1. This is achieved through a process of tessellating child fragments within the outline of the parent iceberg in a manner similar to assembling a jigsaw puzzle (Zhang et al., 2017) but without any image information to assist and in the presence of the potential for substantial portions of the parent to have been lost entirely from the detections due to melt and small scale fracture. We use this process to assess which shapes share similar parts of their geometries and between which it is possible to make legitimate parent-child linkages. The challenge is to match the high frequency components of the perimeter shape while ignoring the global invariances of translation and rotation that arise from iceberg drift between observations. Furthermore, due to melt and small scale calving (below the detection limit) modifying the edges of icebergs, imperfect segmentation recall, and sub-pixel uncertainties in edge position, it is unlikely that there will ever be perfect correspondence between any parts of the perimeter shapes of parent and child icebergs. Similarly, it is unlikely that the total area of children emanating from one parent will exactly match the original area of that parent.

https://doi.org/10.5194/egusphere-2025-2886
Preprint. Discussion started: 7 July 2025

3.3.1 Outline alignment:

The core of the process is an outline alignment step, whereby sub-sections of shape perimeters that are similar between icebergs are used to align potential children to potential parents (Figure 2).

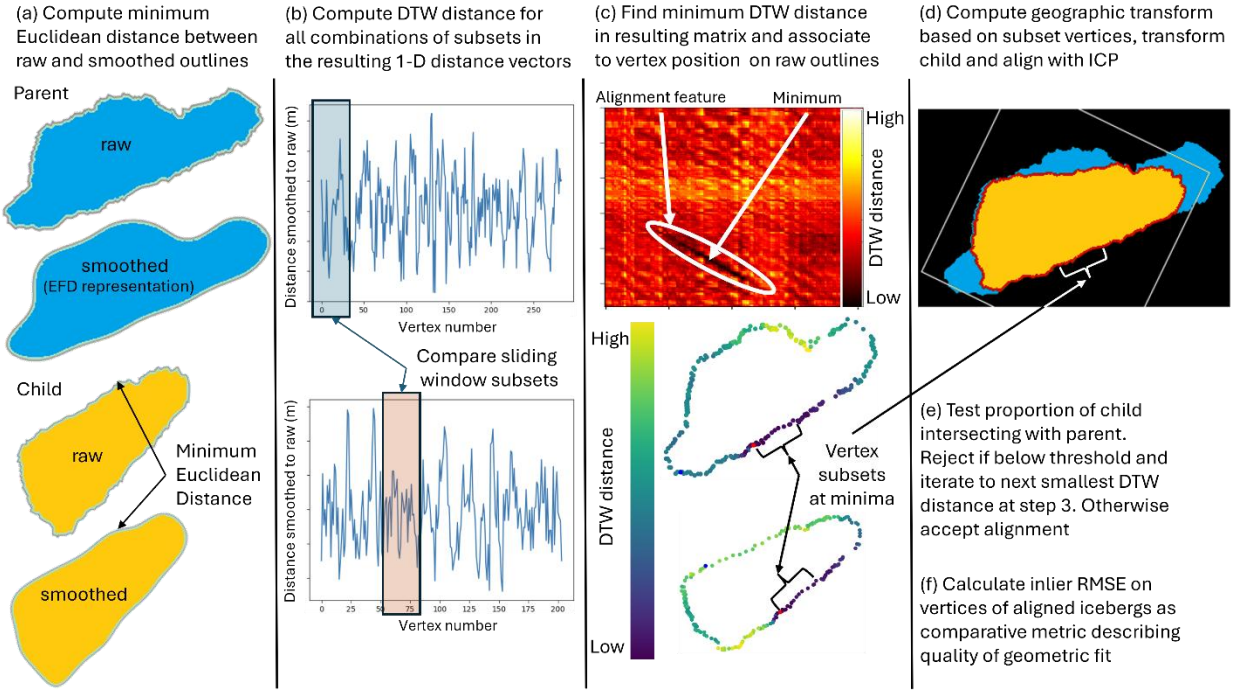

Figure 2: Process for outline alignment of child with parent based on finding minimal dynamic time warping (DTW) distances between high frequency components of perimeter shapes – Represented as Process 4 in Figure 3.

To isolate the high frequency shape components and remove translation and rotation we first smooth the raw perimeter of each shape using a 5th order EFD and reconstruct the shape from the coefficients and centroid. We then take the Euclidean distance from each vertex in the raw perimeter to the nearest point on the smoothed outline. Distances are negative where the raw outline is further from the centroid than the smoothed outline ((a), Figure 2). This produces a 1-dimensional (1-D) vector of deviations between raw and smoothed outlines. We then use dynamic time warping (DTW) to estimate similarity between subset regions of these 1-D vectors using a sliding window approach ((b), Figure 2). DTW is a curve matching algorithm that estimates dissimilarity between sequences as a warping distance, which is low when sequences align well and high when they align poorly. It is widely used in audio, speech and text recognition (Müller, 2007; Myers & Rabiner, 1981) and does not assume correspondences between the vertices of the two sequences. For each pair of sub-sections (in our case each 10 vertices long), we compute a DTW distance using the *dtaidistance* Python package (Meert et al., 2020), producing a matrix of DTW distances, in which areas where the shape perimeters align well are observable as minima ((c), Figure 2). We take the sliding window subsets corresponding to the lowest DTW distance found and use the geographic coordinates of the vertices to compute a least-squares transformation matrix between them. We apply this transformation to the child iceberg to translate and rotate

https://doi.org/10.5194/egusphere-2025-2886
Preprint. Discussion started: 7 July 2025

it, thereby superimposing it on the parent iceberg ((d), Figure 2). We then perform an iterative closest points alignment on all vertices of the parent and aligned child to reconcile any small positional errors. These largely arise from angular errors in the transformation estimation. We impose a heuristic constraint that the alignment must result in more than 96% of the area of the child being within its intersection with the parent ((e), Figure 2). This constrains children to fall largely within the parent geometry. If this constraint is breached we discard the alignment and iterate to the sub-sequences with the second smallest DTW distance, repeating the transformation and overlap checks. This process is repeated for DTW distances below the median of the matrix until a satisfactory alignment is found. If no alignment is found the child is not linked to the parent. Having accepted an alignment we compute the inlier RMSE of the vertex coordinates to represent how good the geometric fit between the outlines is and upon which to compare competing possible alignments ((f), Figure 2).

3.3.2 Tessellation

At any given time step there may be multiple potential parents and children. The alignment process described above for a single parent-child linkage is deployed within an iterative workflow in such circumstances in order to tessellate multiple children within parents (Figure 3).

https://doi.org/10.5194/egusphere-2025-2886
Preprint. Discussion started: 7 July 2025

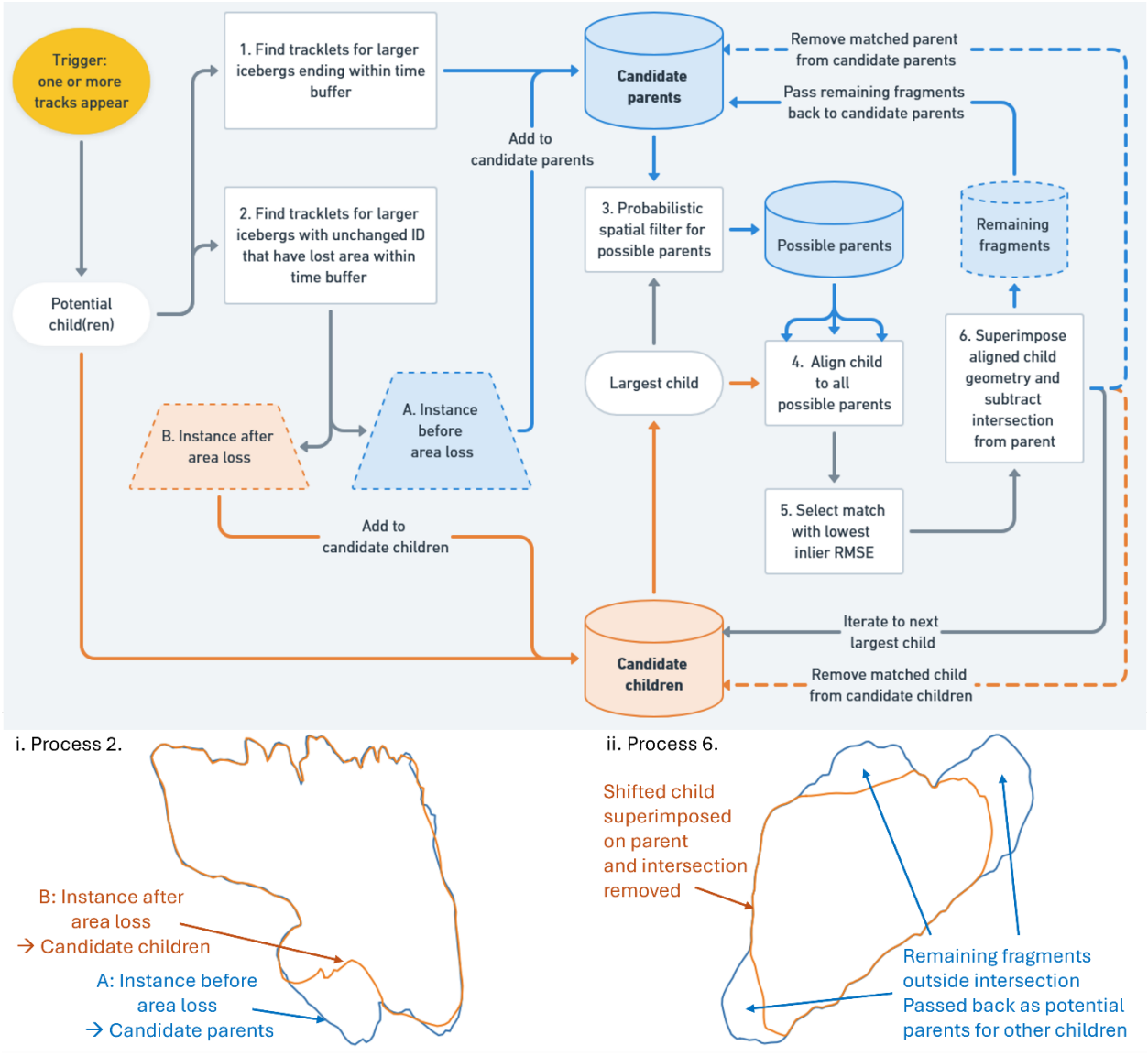

Figure 3: Tessellation workflow for associating multiple parent and child icebergs. Blue denotes parents, orange denotes children. Processes are shown in rectangular boxes. Insets i. and ii. illustrate Processes 2 and 6 respectively. Process 4 corresponds to the outline alignment represented in Figure 2.

The workflow is triggered when a previously unseen iceberg appears (i.e. a new tracklet is initiated). In such situations we require an explanation for the appearance of an iceberg that we have not previously observed and calving from a larger iceberg is the most probable explanation (Barbat et al., 2021), particularly when far from glacier or ice shelf calving fronts (we discuss the limitations of this assumption further below). The potential source could either be an iceberg that has disappeared (a tracklet that has ended, see process 1, Figure 3) or an iceberg that continues to be observed but has lost sufficient area to account for the newly observed iceberg (process 2, Figure 3). In the latter case, the most recent previous observations of such

https://doi.org/10.5194/egusphere-2025-2886
Preprint. Discussion started: 7 July 2025

icebergs are treated as a candidate parents (A, blue, in inset i. of Figure 3) while the corresponding iceberg at the same time point as the track appearance trigger becomes an additional candidate child (B, orange, in inset i. of Figure 3) such that its intersection is removed from the parent A following Process 6 (Figure 3) before testing the newly appeared iceberg for fit to any fragments that remain.

We thus end up with a list of candidate parents and a list of candidate children. Starting with the largest candidate child, we identify possible parents within the preceding time range using a probabilistic spatial filter (process 3, Figure 3) based upon vector fields interpolated from the tracklet data (see supplementary material S1). We perform alignment (Figure 2 and process 4, Figure 3) against all possible larger parents. We take the alignment with the lowest inlier RMSE following iterative closest point (ICP) registration as being the most likely parent-child relationship (process 5, Figure 3). We then remove the intersection of the aligned child's geometry (orange in inset ii. to Figure 3) from that of the parent (blue in inset ii. to Figure 3). This leaves parts of the parent unaccounted for, from which other children could be derived (inset ii. Figure 3). These remaining parts are added back to the candidate parents list while the aligned child is removed from the candidate children list and its parentage recorded and the parent is removed from the candidate parents list, having been accounted for. This process is repeated until all candidate children have been assigned to a parent or there are no more valid alignments found. Candidate children for which no alignment to a parent is found initiate a new lineage.

3.3.3 Lineage reconstruction

The tessellation procedure is conducted across the dataset, iterating by time step. We then enforce rules about how lineages are represented. Icebergs maintain a single identity for as long as no fragmentation event is detected. A fragmentation event is defined as when two or more icebergs share a parent. Consequently, an iceberg may change shape and size substantially while maintaining an identity if no others can be aligned to the parts it loses. Conversely, it may remain substantially the same shape, but if a small fragment calves and is associated with it (as in inset i. Figure 3), both that fragment and the largely unchanged iceberg will be assigned new identities (thereby initiating new tracklets) and their parent attribute set to the initial identity. Parents may be linked to many children but a child may only be linked to one parent. We are thus able to reconstruct the lineage trees of icebergs (Panel C, Figure 1) in an automated fashion for the first time.

3.3.4 Evaluation

To our knowledge, object movement and lineage tracking have not been previously explored in a geospatial context, nor in cases where track branching may result in more than two children, as seen in cell tracking. Consequently, there are no established performance metrics for our context. However, we adapt metrics from the cell tracking domain to assess

https://doi.org/10.5194/egusphere-2025-2886
Preprint. Discussion started: 7 July 2025

CryoTrack's performance. We used the *traccuracy* python package, with a custom data loader to handle geospatial vector formats, to evaluate our outputs against the manually ascribed lineages encoded in the CI2D3 dataset (GT).

We report three transferrable metrics derived from the Cell Tracking Challenge (Ulman et al., 2017): Tracking Accuracy (TRA), Target Effectiveness (TE) and Track Purity (TP). TRA describes how well all objects (icebergs) are both identified and tracked (although in this case there is no detection step). TE describes the proportion of each reference track for which the longest reconstructed track overlaps, averaged over all reference tracks. TP is the inverse of TE, being the proportion of each reconstructed track for which the longest reference track overlaps, averaged over all reconstructed tracks. All three vary in the range 0-1, with 1 being perfect reconstruction of the tracking graph. The reader is referred to Matula et al. (2015) for further detail. In addition to these, we introduce new evaluation metrics tailored to scientific and operational applications of iceberg tracking.

Scientific applications focus on identifying iceberg origins, reconstructing drift trajectories, determining fragmentation timing, and quantifying area loss rates over long timescales, potentially spanning years or decades. Performance in this context depends on whether an iceberg can be correctly linked back to its original source, regardless of where or when it is observed. We define Root Precision (RP) as the proportion of icebergs correctly attributed to their source at their last observed position. Root Area Precision (RAP) extends this by weighting RP according to iceberg area, emphasizing the accuracy of total ice mass attribution.

Operational applications focus on hazard avoidance (Smith et al., 2025), where the priority would be accurately tracking icebergs over shorter timescales (days or weeks) to infer recent trajectories and predict future locations over relatively short timescales. To assess performance in this context, we evaluate how well predicted tracks match ground truth tracks over different time intervals. We report precision (true positives divided by all positives), recall (true positives divided by the sum of true positives and false negatives), and F1-score (harmonic mean of precision and recall) for different lead times, illustrating the reliability of tracks, and therefore trajectories, over those intervals.

Generational (parent-child) linkages between icebergs are assessed based on their agreement with the ground truth dataset. Since icebergs can divide into more than two fragments, these relationships are evaluated independently rather than requiring a strict two-child split, as in cell tracking literature. Generational linkages in the predicted set may also be represented by tracklets in a continuous track in the GT set, and vice versa. Such linkages themselves are also treated as true positives since they link the correct two objects, although they do imply either commission or omission of another generational linkage at the same stage. Division Precision (DP), Division Recall (DR), and Division F1-score (DF-1) measure the accuracy of these generational linkages.

We anticipated tracking to be most challenging in the congested areas close to the calving front of Petermann Galcier. This is particularly true because the dataset currently does not allow for the glacier to be represented as a potential source of newly observed icebergs. To investigate the effect of near-glacier confusion we also evaluated performance for a subset that excludes the fjord (see Appendix B: Exclusion of fjord for method).

https://doi.org/10.5194/egusphere-2025-2886
Preprint. Discussion started: 7 July 2025

4 Results

4.1 Iceberg lineages:

We tested a variety of combinations of parameters for the generational linking stage, observing the expected trade-offs between precision and recall as we varied the effective search radius defined by the sigma and probability threshold parameters (larger search domain increases precision and decreases recall, and *vice versa*). Allowing lower proportions of overlap when matching shapes leads to less well constrained matches, reducing precision while meaning that the shapes of remaining fragments for tessellation of smaller icebergs are less robust, decreasing recall. Lengthening or shortening the time buffer tends to decrease precision but is a function of the temporal sparsity of observations in the domain so is informed by the dataset structure. Lengthening the sub-section length for the DTW distance matrix comparison adds computational complexity and reduces performance for the smaller icebergs with fewer perimeter vertices while shortening it reduces the information available for DTW calculation too much. We did not observe any extreme, abrupt or unexpected sensitivity to any of the configurable parameters during our tests. The final configuration for which we report performance used the following parameters: sigma = 5000; probability threshold = 0.05; proportional overlap = 0.96; time buffer = 6; sub-section length = 10. Examples of lineages reconstructed using our method are shown in Figure 4. The main panel shows iceberg tracks and identities in a spatial context, viewed obliquely such that the track history through time is represented as height above the basemap surface. The inset panel shows the lineage graph of the iceberg indicated by the yellow arrow and the horizontal line on the inset indicates the time point of the main pane observation.

https://doi.org/10.5194/egusphere-2025-2886
Preprint. Discussion started: 7 July 2025

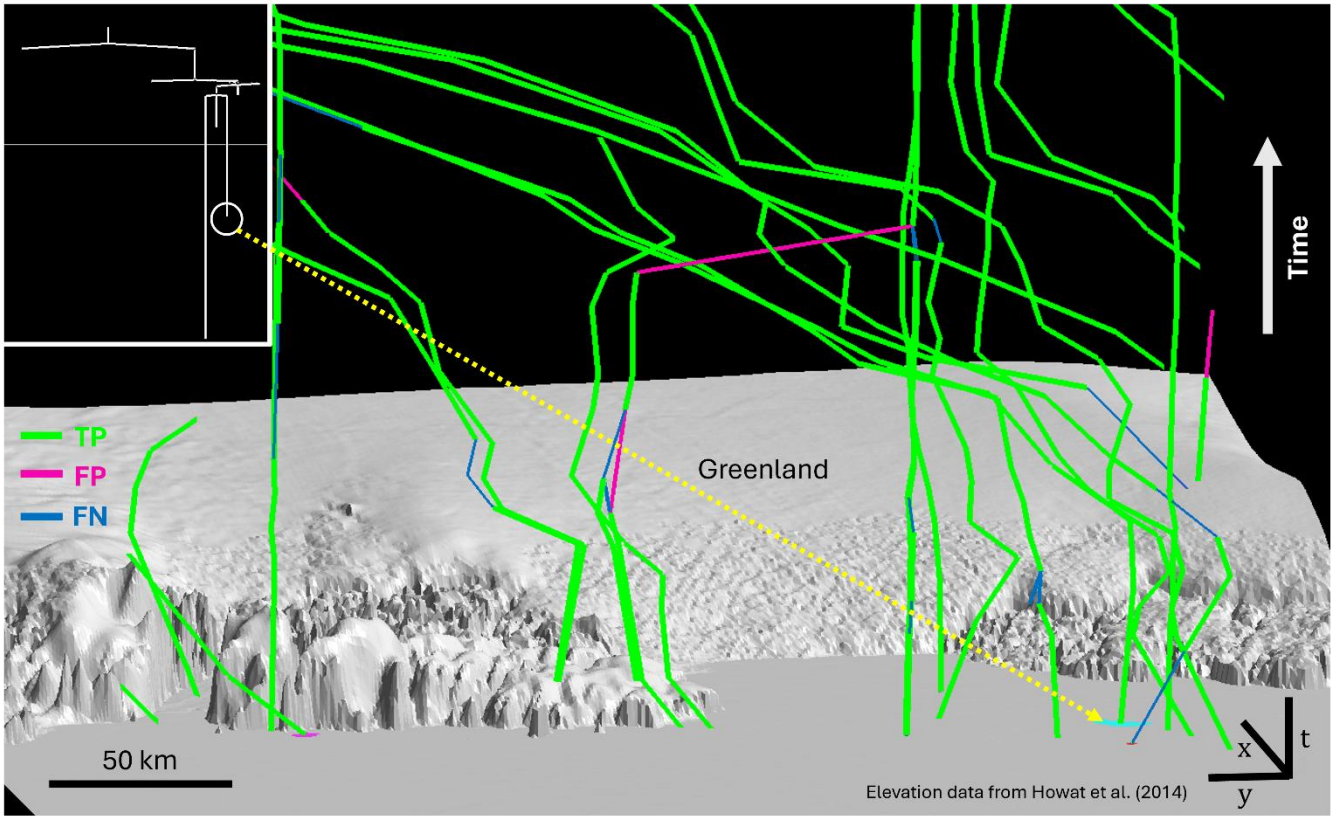

Figure 4: Example tracks reconstructed from the CI2D3 dataset showing true positive (TP), false positive (FP) and false negative (FN) links. Top left inset shows lineage tree for the iceberg indicated by the yellow dashed arrow. Time is represented as height from the meshed Greenland elevation data surface, such that tracks towards the top of the figure represent iceberg locations further back in time, with the most recent observation coinciding with sea level. Greenland elevation data from GIMP-DEM 90 (Howat et al., 2014).

4.2 Performance:

Performance, as evaluated against the metrics described in Sect. 3.3.4, is reported in Table 1. The tracker exhibits strong performance overall, with tracks closely reflecting the manually annotated ones with high overall accuracy and long periods of perfect track overlap, particularly between fragmentation events. Fragmentation is captured less well but demonstrates good performance given its novelty and presents clear avenues for future improvement.

Table 1 - Tracker performance

Metric	Full study domain	Domain excluding fjord
Tracking Accuracy (TRA)	0.98	0.99
Target Effectiveness (TE)	0.72	0.83

https://doi.org/10.5194/egusphere-2025-2886
Preprint. Discussion started: 7 July 2025

Track Purity (TP)	0.87	0.88
Root Precision (RP)	0.51	0.61
Root Area Precision (RAP)	0.94	0.96
Division precision (DP)	0.38	0.70
Division Recall (DR)	0.35	0.34
Division F1-score (DF-1)	0.37	0.46

The discrepancy between RP and RAP arises from the size distribution of icebergs within the dataset and differential tracking performance for different sized icebergs. The relationship between RP and the size of the tracked iceberg is illustrated in Figure 5a (blue bars), where the grey histogram illustrates the frequency of icebergs within each size class. Icebergs are grouped by order of magnitude of surface area, an approach that reflects the size categories proposed by Wesche & Dierking (2015). RP is high for the larger size classes, decreasing as iceberg surface area declines.

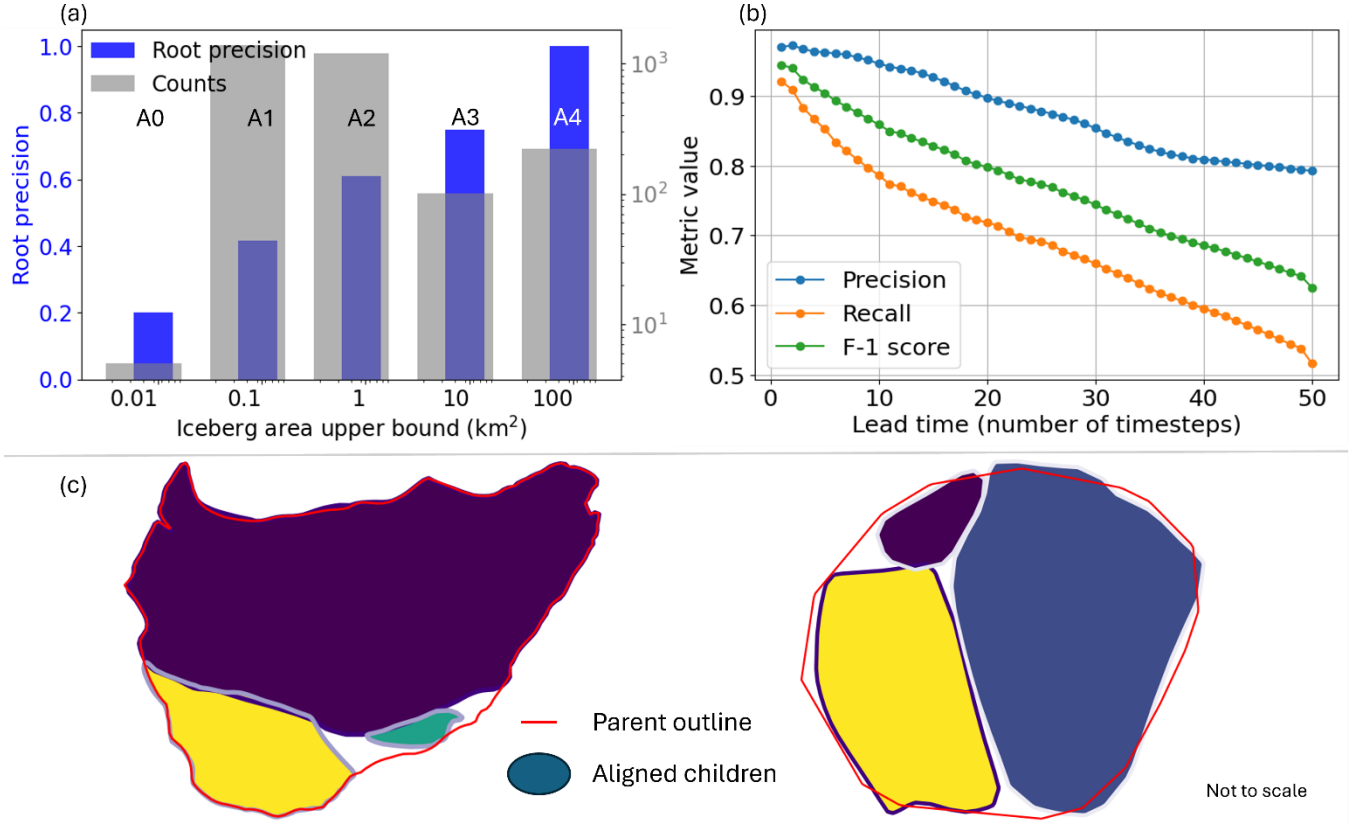

https://doi.org/10.5194/egusphere-2025-2886
Preprint. Discussion started: 7 July 2025

Figure 5: (a) Root precision (blue) by size class of iceberg with size classes A0-A4 following Wesche & Dierking (2015)**, histogram of iceberg observations (grey). (b) Performance in maintaining iceberg identity over 50 time intervals. (c) examples of automated tessellations (not to scale), arbitrary colours with contrasting outlines to illustrate where fitted shapes overlap.**

Performance, as it relates to navigational uses, was strong, with precision, recall and F1-score for maintaining correct iceberg identities across all single observational time intervals of 0.97, 0.90 and 0.93 respectively. Performance remains strong, with F1-score exceeding 0.75, out to lead times of 30 time steps as shown in Figure 5 (b).

Performance in establishing generational linkages is weaker than for other aspects. Our geometric assembly method achieved a Division Precision of 0.39, Division Recall of 0.35 and Division F1-score of 0.37. Overall performance improved when the fjord area was excluded, this being driven by a substantial increase in DP to 0.70, bringing DF-1 to 0.46 despite a small drop in DR (0.34). Examples of tessellations enabling reconstruction of complex many-to-one generational associations are shown in Figure 5c.

5 Discussion

Our proposed method exhibits good performance when evaluated using metrics derived from the Cell Tracking Challenge (CTC) (Ulman et al., 2017). The TRA performance of 0.98 is artificially elevated since the metric includes a component of detection performance. We use the same detections for tracking and evaluation, which implies perfect detection. Nevertheless, this metric may serve as a useful benchmark for future studies applying similar methodologies to tracking objects in machine learning derived segmentations for which independent reference data are available. The values of TE and TP (0.72 and 0.87 respectively) imply that we typically achieve overlap between reconstructed and reference tracks for substantial portions of their lengths.

Our custom metrics derived to support expected scientific downstream applications (RP and RAP) show that we successfully track the vast majority of large icebergs (classes A3 and A4) such that we can correctly identify their source. For smaller icebergs (A0-A2), that ability declines, although for A1 and A2 sizes, moderate performance is still achieved. This decline is to be expected since there is less geometric information available (shorter perimeters and less scope for natural shape variability) to discriminate smaller icebergs from each other while they are also more numerous, which increases the chances of confusion. A4 was the largest class of iceberg represented in the CI2D3 dataset, but is approximately the smallest size of iceberg that would currently be named and tracked in an Antarctic context. Most named icebergs in the Antarctic are in the order 10^{10} m^2 (class A5), with the largest iceberg on record, B15, being in the order 10^{11} m^2. Consequently, our results on the CI2D3 dataset give us confidence that our method would perform well on named Antarctic icebergs as well as substantially smaller ones that are currently not routinely monitored, dramatically increasing the potential number that can be tracked and allowing for a much more comprehensive representation of the diaspora of icebergs originating from continental sources.

https://doi.org/10.5194/egusphere-2025-2886
Preprint. Discussion started: 7 July 2025

We can relate, on average, over 90% of the area of icebergs back to their source when tracklets end. This implies that we are capturing the spatial distribution of most of the ice volume following large calving events (likely greater than the RAP value due to the 3-dimensional geometry of icebergs (Sulak et al., 2017)) and are able to attribute it to particular ice shelves or glaciers. This will allow us to make inferences regarding the distal impacts of changes in ice stream velocity or calving behaviour at specific locations around the coasts of either Greenland or Antarctica that may be forecast by numerical ice sheet simulations.

For operational contexts where recent motion is more informative than provenance we demonstrate a strong ability to maintain the correct identity of icebergs across multiple time intervals. The F1-score of our tracker exceeds 0.90 for lead times up to five intervals, which equates to approximately two months for the target observation frequency of the CI2D3 dataset, and remains above 0.75 to 30 intervals (approximately 1 year, (b) Figure 5). This performance provides a robust foundation for characterising iceberg motion recent to any given observation and informing inference (either human or machine-generated) about future drift patterns. Such insight represents a valuable decision support asset for navigation and hazard mitigation for fixed and mobile maritime infrastructure.

Establishing robust generational linkages is the most challenging part of the proposed tracking scheme. This is reflected in the DP, DR, and DF-1, which are lower than for the other metrics. The generational linkage procedure presented (Figure 2, Figure 3) demonstrates a clear ability to correctly align multiple child icebergs within their parent ((c), Figure 5) and captures a reasonable proportion of fragmentations correctly (Table 1). This is a unique capability for an automated tracking system, the performance of which will be improved upon in future work. A primary limitation of the generational matching is its greedy character that is not currently balanced by awareness of potential sources other than existing icebergs (such as calving fronts), or fates other than fragmentation (such as drifting beyond domain boundaries). This leads to erroneous linkages being made, particularly near the calving tongue of Petermann Glacier and at domain boundaries more generally. The problem could be mitigated by including the geometry of the calving tongue as a potential parent object within the tracking scheme such that newly calved icebergs could be matched to a change in calving front geometry. This would also help enhance our ability to track ice volumes right back to their sources. This was not possible in this study, using the CI2D3 dataset, because the calving front was not digitized and the underlying imagery were not available. When the fjord area was excluded (Appendix B: Exclusion of fjord) tracker performance generally improved (Table 1) which implies that incorporating calving sources could substantially improve full lineage reconstructions.

Icebergs may also appear after drifting from distal sources across the study domain boundary, while tracks may also end when icebergs drift outside the domain. In the btrack optimization step (not used here as it is reliant upon the motion model which was disabled), hypotheses are tested that include appearance or disappearance across scene boundaries based on proximity and trajectory. Future work will implement probabilistic matching across all feasible associations based on the likelihood of geometric matches compared against the likelihood of alternative sources and fates by constructing spatial priors, like those

https://doi.org/10.5194/egusphere-2025-2886
Preprint. Discussion started: 7 July 2025

generated for spatial filtering of potential parents (Appendix A: Probabilistic spatial filter for constraining possible parent icebergs:).

In the geospatial context of this study, the domain spans many smaller, asynchronous image volume acquisitions such that many image footprints taken at different times combine to make up the domain. The consequence of this is that at any one time where some part of the domain is observed, most of the domain is unobserved. The naïve treatment of the time domain in this study stacks observations and assigns unique timesteps to every point at which valid data are acquired anywhere in the domain. Therefore, for any given point in the domain, the temporal sequence of valid observations is sparse. This is the principal cause of the need for a time buffer, and for that time buffer to be relatively long (6 timesteps). As the domain gets larger, the sparsity of observations at any given location becomes more acute. This motivated the selection of a relatively small subset of the total dataset extent around the main calving fronts while retaining the majority of lineages. Nevertheless, a more sophisticated schema for handling the representation and tracking of moving objects in an asynchronously acquired domain is required if larger domains are to be studied. This problem is encountered in other domains and development of a generalized solution is beyond the scope of this study but offers an opportunity for collaboration across research disciplines.

Central to our contribution is a novel generalizable geometric assembly algorithm suited to geospatial contexts, capable of tessellating shapes to reconstruct other, larger geometries in the presence of large global invariances and imperfect correspondences between vertices. This approach should operate in any context where shapes have characteristic, high frequency, perimeter curves, although tuning of the smoothing and sliding window parameters is likely to be necessary, including when applying it to machine-generated iceberg segmentations. Applications include tracking of ice floes or reassembly of archaeological artefacts. Unlike pictorial jigsaw puzzle assembly approaches (Markaki & Panagiotakis, 2023; Shen et al., 2018), our method does not rely on any textural or image data, so is potentially more broadly applicable where only segmentation masks or silhouettes are available.

Future work will apply the approach to machine-generated segmentations and evaluate performance in an Antarctic context, then apply the tracker at a continental scale to underpin future freshwater distribution and mechanistic calving models. There is also scope for exploring supervised tracking and fragment assembly algorithms. The underlying SAR image data were not available to the authors for the purposes of this work, but if imagery corresponding to the masks in CI2D3 were available, this would offer the chance to explore supervised methods such as the transformer based cell tracking package Trackastra (Gallusser & Weigert, 2025).

6 Conclusions

We present a novel geospatial tracking approach for monitoring and reconstructing tracks and lineages of icebergs, evaluated against a large, unique manually annotated dataset of icebergs originating from Greenland ice tongues. We extend previous work attempting to track icebergs (Barbat et al., 2021; Koo et al., 2023; Koo et al., 2021) by developing a fully automated, unsupervised tracking methodology that establishes linkages between icebergs across fragmentation events, thus enabling

https://doi.org/10.5194/egusphere-2025-2886
Preprint. Discussion started: 7 July 2025

reconstruction of lineage trees and full drift paths that can be traced back to the initial calving location even if the iceberg has broken up in the interim. We provide extensive evaluation of the tracker's performance using generalized metrics and those tailored to the expected downstream use cases for enhanced iceberg monitoring. This opens new opportunities to understand iceberg drift and deterioration at scale, improve iceberg motion, melt and fragmentation models as well as predict distal impacts of calving events in a much more granular manner than has hitherto been possible. The geometric assembly approach is theoretically transferrable to other domains while the whole tracking pipeline is also suited to geometry based geospatial tracking problems. The CryoTrack code is available at https://github.com/lupinthief/CryoTrack.

Author contributions

BE developed the methodology and code and prepared the manuscript with contributions from all authors. AL developed tracking functionality for Btrack to enable this work and advised on approach. AC assisted in data provision, design and manuscript preparation. AF and SH conceived the work and assisted in methodological design and manuscript preparation.

Code and data availability

The CryoTrack code is available at https://github.com/lupinthief/CryoTrack. The CI2D3 database is available at https://www.polardata.ca/pdcsearch/PDCSearch.jsp?doi_id=12678

Competing interests

The authors declare that they have no conflict of interest

Acknowledgements

This work was funded by EPSRC Grant EP/Y028880/1, The Alan Turing Institute, and the Polar Science for a Sustainable Planet programme at the British Antarctic Survey. We are grateful for productive discussions with, among others, Martin Rogers, Louisa Van Zeeland, Ellen Bowler, Arianna Salili-James, Cameron Trotter, Andreas Bock, James Byrne and Jonathan Smith. GitHub Copilot was used during code development.

https://doi.org/10.5194/egusphere-2025-2886
Preprint. Discussion started: 7 July 2025

References

Ackermann, L., Rackow, T., Himstedt, K., Gierz, P., Knorr, G., & Lohmann, G. (2024). A comprehensive Earth system model (AWI-ESM2.1) with interactive icebergs: Effects on surface and deep-ocean characteristics. *Geoscientific Model Development*, *17*(8), 3279–3301. https://doi.org/10.5194/GMD-17-3279-2024

Arrigo, K. R., Van Dijken, G. L., Ainley, D. G., Fahnestock, M. A., & Markus, T. (2002). Ecological impact of a large Antarctic iceberg. *Geophysical Research Letters*, *29*(7), 8-1-8–4. https://doi.org/10.1029/2001GL014160

Bamber, J. L., Tedstone, A. J., King, M. D., Howat, I. M., Enderlin, E. M., van den Broeke, M. R., & Noel, B. (2018). Land Ice Freshwater Budget of the Arctic and North Atlantic Oceans: 1. Data, Methods, and Results. *Journal of Geophysical Research: Oceans*, *123*(3), 1827–1837. https://doi.org/10.1002/2017JC013605

Bamber, J., Van Den Broeke, M., Ettema, J., Lenaerts, J., & Rignot, E. (2012). Recent large increases in freshwater fluxes from Greenland into the North Atlantic. *Geophysical Research Letters*, *39*(19), 19501. https://doi.org/10.1029/2012GL052552

Barbat, M. M., Rackow, T., Wesche, C., Hellmer, H. H., & Mata, M. M. (2021). Automated iceberg tracking with a machine learning approach applied to SAR imagery: A Weddell sea case study. *ISPRS Journal of Photogrammetry and Remote Sensing*, *172*, 189–206. https://doi.org/10.1016/J.ISPRSJPRS.2020.12.006

Barbat, M. M., Wesche, C., Werhli, A. V., & Mata, M. M. (2019). An adaptive machine learning approach to improve automatic iceberg detection from SAR images. *ISPRS Journal of Photogrammetry and Remote Sensing*, *156*, 247–259. https://doi.org/10.1016/J.ISPRSJPRS.2019.08.015

Budge, J. S., & Long, D. G. (2018). A Comprehensive Database for Antarctic Iceberg Tracking Using Scatterometer Data. *IEEE Journal of Selected Topics in Applied Earth Observations and Remote Sensing*, *11*(2), 434–442. https://doi.org/10.1109/JSTARS.2017.2784186

Cenedese, C., & Straneo, F. (2023). Icebergs Melting. *Annual Review of Fluid Mechanics*, *55*(Volume 55, 2023), 377–402. https://doi.org/10.1146/ANNUREV-FLUID-032522-100734/CITE/REFWORKS

Chu, P., Wang, J., You, Q., Ling, H., & Liu, Z. (n.d.). *TransMOT: Spatial-Temporal Graph Transformer for Multiple Object Tracking*.

Crawford, A., Crocker, G., Mueller, D., Desjardins, L., Saper, R., & Carrieres, T. (2018). The Canadian Ice Island Drift, Deterioration and Detection (CI2D3) Database. *Journal of Glaciology*, *64*(245), 517–521. https://doi.org/10.1017/JOG.2018.36

Crawford, A. J., Crocker, G., Smith, J., Mueller, D., & Wagner, T. J. W. (2024). Evaluating the importance of footloose-type failure in ice island deterioration modeling. *Cold Regions Science and Technology*, *228*, 104325. https://doi.org/10.1016/J.COLDREGIONS.2024.104325

https://doi.org/10.5194/egusphere-2025-2886
Preprint. Discussion started: 7 July 2025

Crawford, A. J., Mueller, D., Desjardins, L., & Myers, P. G. (2018). The Aftermath of Petermann Glacier Calving Events (2008–2012): Ice Island Size Distributions and Meltwater Dispersal. *Journal of Geophysical Research: Oceans*, *123*(12), 8812–8827. https://doi.org/10.1029/2018JC014388

Crawford, A. J., Wadhams, P., Wagner, T. J. W., Stern, A., Abrahamsen, E. P., Church, I., Bates, R., & Nicholls, K. W. (2016). Journey of an Arctic ice island. *Oceanography*, *29*(2), 254–263. https://doi.org/10.5670/oceanog.2016.30

Depoorter, M. A., Bamber, J. L., Griggs, J. A., Lenaerts, J. T. M., Ligtenberg, S. R. M., Van Den Broeke, M. R., & Moholdt, G. (2013). Calving fluxes and basal melt rates of Antarctic ice shelves. *Nature 2013 502:7469*, *502*(7469), 89–92. https://doi.org/10.1038/nature12567

Enderlin, E. M., Hamilton, G. S., Straneo, F., & Sutherland, D. A. (2016). Iceberg meltwater fluxes dominate the freshwater budget in Greenland's iceberg-congested glacial fjords. *Geophysical Research Letters*, *43*(21), 11,287-11,294. https://doi.org/10.1002/2016GL070718

England, M. R., Wagner, T. J. W., & Eisenman, I. (2020). Modeling the breakup of tabular icebergs. *Science Advances*, *6*(51). https://doi.org/10.1126/SCIADV.ABD1273

Evans, B., Faul, A., Fleming, A., Vaughan, D. G., & Hosking, J. S. (2023). Unsupervised machine learning detection of iceberg populations within sea ice from dual-polarisation SAR imagery. *Remote Sensing of Environment*, *297*, 113780. https://doi.org/10.1016/J.RSE.2023.113780

Fuglem, M., & Jordaan, I. (2017). Risk Analysis and Hazards of Ice Islands. *Springer Polar Sciences*, 395–415. https://doi.org/10.1007/978-94-024-1101-0_15

Gallusser, B., & Weigert, M. (2025). TRACKASTRA: Transformer-Based Cell Tracking for Live-Cell Microscopy. *Lecture Notes in Computer Science (Including Subseries Lecture Notes in Artificial Intelligence and Lecture Notes in Bioinformatics)* , *15134 LNCS*, 467–484. https://doi.org/10.1007/978-3-031-73116-7_27

Hill, B. T. (2001). Ship collisions with icebergs: an historical record of collisions in the seas around North America and Greenland. *Proceedings of the 16th International Conference on Ports and Ocean Engineering under Arctic Conditions.*, 10.

Howat, I. M., Negrete, A., & Smith, B. E. (2014). The Greenland Ice Mapping Project (GIMP) land classification and surface elevation data sets. *The Cryosphere*, *8*, 1509–1518. https://doi.org/10.5194/tc-8-1509-2014

Huth, A., Adcroft, A., & Sergienko, O. (2022). Parameterizing Tabular-Iceberg Decay in an Ocean Model. *Journal of Advances in Modeling Earth Systems*, *14*(3), e2021MS002869. https://doi.org/10.1029/2021MS002869

Huth, A., Adcroft, A., Sergienko, O., & Khan, N. (2022). Ocean currents break up a tabular iceberg. *Science Advances*, *8*(42), 6974. https://doi.org/10.1126/SCIADV.ABQ6974/SUPPL_FILE/SCIADV.ABQ6974_MOVIE_S1.ZIP

Koo, Y. H., Xie, H., Ackley, S. F., Mestas-Nuñez, A. M., Macdonald, G. J., & Hyun, C. U. (2021). Semi-automated tracking of iceberg B43 using Sentinel-1 SAR images via Google Earth Engine. *Cryosphere*, *15*(10), 4727–4744. https://doi.org/10.5194/TC-15-4727-2021

https://doi.org/10.5194/egusphere-2025-2886
Preprint. Discussion started: 7 July 2025

Koo, Y., Xie, H., Mahmoud, H., Iqrah, J. M., & Ackley, S. F. (2023). Automated detection and tracking of medium-large icebergs from Sentinel-1 imagery using Google Earth Engine. *Remote Sensing of Environment*, *296*, 113731. https://doi.org/10.1016/J.RSE.2023.113731

Kuhl, F. P., & Giardina, C. R. (1982). Elliptic Fourier features of a closed contour. *Computer Graphics and Image Processing*, *18*(3), 236–258. https://doi.org/10.1016/0146-664X(82)90034-X

Markaki, S., & Panagiotakis, C. (2023). Jigsaw puzzle solving techniques and applications: a survey. *Visual Computer*, *39*(10), 4405–4421. https://doi.org/10.1007/S00371-022-02598-9/FIGURES/12

Marsh, R., Ivchenko, V. O., Skliris, N., Alderson, S., Bigg, G. R., Madec, G., Blaker, A. T., Aksenov, Y., Sinha, B., Coward, A. C., Le Sommer, J., Merino, N., & Zalesny, V. B. (2015). NEMO-ICB (v1.0): Interactive icebergs in the NEMO ocean model globally configured at eddy-permitting resolution. *Geoscientific Model Development*, *8*(5), 1547–1562. https://doi.org/10.5194/GMD-8-1547-2015

Marson, J. M., Myers, P. G., Hu, X., & Le Sommer, J. (2018). Using Vertically Integrated Ocean Fields to Characterize Greenland Icebergs' Distribution and Lifetime. *Geophysical Research Letters*, *45*(9), 4208–4217. https://doi.org/10.1029/2018GL077676

Matula, P., Maska, M., Sorokin, D. V., Matula, P., Ortiz-De-Solórzano, C., & Kozubek, M. (2015). Cell Tracking Accuracy Measurement Based on Comparison of Acyclic Oriented Graphs. *PLOS ONE*, *10*(12), e0144959. https://doi.org/10.1371/JOURNAL.PONE.0144959

McInnes, L., Healy, J., & Melville, J. (2018). *UMAP: Uniform Manifold Approximation and Projection for Dimension Reduction*. https://arxiv.org/abs/1802.03426v3

Meert, W., Hendrickx, K., Van Craenendonck, T., Robbrechts, P., Blockeel, H., & Davis, J. (2020). *DTAIDistance* (2). https://github.com/wannesm/dtaidistance.

Meinhardt, T., Kirillov, A., Leal-Taixé, L., & Feichtenhofer, C. (n.d.). *TrackFormer: Multi-Object Tracking with Transformers*. Retrieved July 8, 2024, from https://github.

Morison, J., & Goldberg, D. (2012). A brief study of the force balance between a small iceberg, the ocean, sea ice, and atmosphere in the Weddell Sea. *Cold Regions Science and Technology*, *76–77*, 69–76. https://doi.org/10.1016/J.COLDREGIONS.2011.10.014

Moyer, A. N., Sutherland, D. A., Nienow, P. W., & Sole, A. J. (2019). Seasonal Variations in Iceberg Freshwater Flux in Sermilik Fjord, Southeast Greenland From Sentinel-2 Imagery. *Geophysical Research Letters*, *46*(15), 8903–8912. https://doi.org/10.1029/2019GL082309

Mueller, D. R., Crawford, A., Copland, L., & Van Wychen, W. (2013). *Ice island and iceberg fluxes from Canadian High Arctic sources (Contract Report No. Final Draft Report).*

Müller, M. (2007). Dynamic Time Warping. In Information Retrieval for Music and Motion, chapter 4, pages 69-84. *Information Retrieval for Music and Motion*, 1–313.

https://doi.org/10.5194/egusphere-2025-2886
Preprint. Discussion started: 7 July 2025

https://www.springer.com/cda/content/document/cda_downloaddocument/9783540740476-1.pdf?SGWID=0-0-45-452103-p173751818

Myers, C. S., & Rabiner, L. R. (1981). A Comparative Study of Several Dynamic Time-Warping Algorithms for Connected-Word Recognition. *Bell System Technical Journal*, *60*(7), 1389–1409. https://doi.org/10.1002/J.1538-7305.1981.TB00272.X

Rignot, E., Jacobs, S., Mouginot, J., & Scheuchl, B. (2013). Ice-shelf melting around antarctica. *Science*, *341*(6143), 266–270. https://doi.org/10.1126/SCIENCE.1235798/SUPPL_FILE/RIGNOT.SM.PDF

Sackinger, W. M., Shoemaker, H. D., Serson, H., Jefferies, M. O., & Yan, M.-H. (1985). Ice islands as hazards to Arctic offshore production structures,. *The 17th Annual Offshore Technology Conference.* .

Shen, B., Zhang, W., Zhao, H., Jin, Z., & Wu, Y. (2018). *Solving Pictorial Jigsaw Puzzle by Stigmergy-inspired Internet-based Human Collective Intelligence*. http://arxiv.org/abs/1812.02559

Shiggins, C. J., Lea, J. M., & Brough, S. (2023). Automated ArcticDEM iceberg detection tool: insights into area and volume distributions, and their potential application to satellite imagery and modelling of glacier-iceberg-ocean systems. *Cryosphere*, *17*(1), 15–32. https://doi.org/10.5194/TC-17-15-2023

Silva, T. A. M., & Bigg, G. R. (2005). Computer-based identification and tracking of Antarctic icebergs in SAR images. *Remote Sensing of Environment*, *94*(3), 287–297. https://doi.org/10.1016/J.RSE.2004.10.002

Smith, J., Hall, S., Coombs, G., Abbot, H., Fekry, A., Thorne, M. A. S., Long, D., & Fox, M. (2025). Path-Planning on a Spherical Surface with Disturbances and Exclusion Zones. *Journal of Artificial Intelligence Research*, *82*, 1845–1907. https://doi.org/10.1613/JAIR.1.16746

Smith, K. L., Sherman, A. D., Shaw, T. J., & Sprintall, J. (2013). Icebergs as unique Lagrangian ecosystems in polar seas. *Ann. Rev. Mar. Sci.*, *5*, 269–287. https://doi.org/10.1146/annurev-marine-121211-172317

Smith, R. S., Mathiot, P., Siahaan, A., Lee, V., Cornford, S. L., Gregory, J. M., Payne, A. J., Jenkins, A., Holland, P. R., Ridley, J. K., & Jones, C. G. (2021). Coupling the U.K. Earth System Model to Dynamic Models of the Greenland and Antarctic Ice Sheets. *Journal of Advances in Modeling Earth Systems*, *13*(10), e2021MS002520. https://doi.org/10.1029/2021MS002520

Stern, A. A., Adcroft, A., & Sergienko, O. (2016). The effects of Antarctic iceberg calving-size distribution in a global climate model. *Journal of Geophysical Research: Oceans*, *121*(8), 5773–5788. https://doi.org/10.1002/2016JC011835

Sulak, D. J., Sutherland, D. A., Enderlin, E. M., Stearns, L. A., & Hamilton, G. S. (2017). Iceberg properties and distributions in three Greenlandic fjords using satellite imagery. *Annals of Glaciology*, *58*(74), 92–106. https://doi.org/10.1017/AOG.2017.5

Sun, P., Cao, J., Jiang, Y., Zhang, R., Xie, E., Yuan, Z., Wang, C., & Luo, P. (2020). *TransTrack: Multiple Object Tracking with Transformer*. https://arxiv.org/abs/2012.15460v2

Tournadre, J., Bouhier, N., Girard-Ardhuin, F., & Rémy, F. (2015). Large icebergs characteristics from altimeter waveforms analysis. *Journal of Geophysical Research: Oceans*, *120*(3), 1954–1974. https://doi.org/10.1002/2014JC010502

https://doi.org/10.5194/egusphere-2025-2886
Preprint. Discussion started: 7 July 2025

Tournadre, J., Bouhier, N., Girard-Ardhuin, F., & Rémy, F. (2016). Antarctic icebergs distributions 1992-2014. *Journal of Geophysical Research: Oceans*, *121*(1), 327–349. https://doi.org/10.1002/2015JC011178

Ulicna, K., Vallardi, G., Charras, G., & Lowe, A. R. (2021). Automated Deep Lineage Tree Analysis Using a Bayesian Single Cell Tracking Approach. *Frontiers in Computer Science*, *3*, 92. https://doi.org/10.3389/FCOMP.2021.734559/BIBTEX

Ulman, V., Maška, M., Magnusson, K. E. G., Ronneberger, O., Haubold, C., Harder, N., Matula, P., Matula, P., Svoboda, D., Radojevic, M., Smal, I., Rohr, K., Jaldén, J., Blau, H. M., Dzyubachyk, O., Lelieveldt, B., Xiao, P., Li, Y., Cho, S. Y., … Ortiz-De-Solorzano, C. (2017). An objective comparison of cell-tracking algorithms. *Nature Methods 2017 14:12*, *14*(12), 1141–1152. https://doi.org/10.1038/nmeth.4473

Virtanen, P., Gommers, R., Oliphant, T. E., Haberland, M., Reddy, T., Cournapeau, D., Burovski, E., Peterson, P., Weckesser, W., Bright, J., van der Walt, S. J., Brett, M., Wilson, J., Millman, K. J., Mayorov, N., Nelson, A. R. J., Jones, E., Kern, R., Larson, E., … Vázquez-Baeza, Y. (2020). SciPy 1.0: fundamental algorithms for scientific computing in Python. *Nature Methods*, *17*(3), 261–272. https://doi.org/10.1038/S41592-019-0686-2

Wagner, T. J. W., Dell, R. W., & Eisenman, I. (2017). An analytical model of iceberg drift. *J. Phys. Oceanogr.*, *47*(7), 1605–1616. https://doi.org/10.1175/jpo-d-16-0262.1

Wesche, C., & Dierking, W. (2015). Near-coastal circum-Antarctic iceberg size distributions determined from Synthetic Aperture Radar images. *Remote Sensing of Environment*, *156*, 561–569. https://doi.org/10.1016/J.RSE.2014.10.025

Zeinali-Torbati, R., Turnbull, I. D., Taylor, R. S., & Mueller, D. (2021). A probabilistic model for fracture events of Petermann ice islands under the influence of atmospheric and oceanic conditions. *Cryosphere*, *15*(12), 5601–5621. https://doi.org/10.5194/TC-15-5601-2021

Zhang, M., Chen, S., Shu, Z., Xin, S. Q., Zhao, J., Jin, G., Zhang, R., & Beyerer, J. (2017). Fast algorithm for 2d fragment assembly based on partial emd. *Vis. Comput.*, *33*(12), 1601–1612. https://doi.org/10.1007/s00371-016-1303-3

Appendix A: Probabilistic spatial filter for constraining possible parent icebergs:

The search domain for potential parent icebergs when conducting the generational linkage stage is constrained by vector fields learned from the tracklets generated for unchanged iceberg identities and the time-lag between observations of the child and potential parent icebergs.

Tracklets are initially temporally densified such that each arc represents a single time step. This is achieved by linear interpolation of the iceberg locations between start and end point for cases where an arc's duration is greater than one time interval. Radial Basis Function interpolation (scipy.interpolation.RBFInterpolator ((Virtanen et al., 2020), linear kernel, smoothing 1e5) is then applied to the tracklet arcs with uniform time duration (1) and predicted onto a 25 by 25 grid covering

https://doi.org/10.5194/egusphere-2025-2886
Preprint. Discussion started: 7 July 2025

the study domain to produce vector fields describing the interpolated motion of icebergs dependent on their location within the domain (vx and vy). These are shown in Figure A1.

When constraining potential parents for a child iceberg, probabilistic fields of source location are generated by 'backtracking' through the vector fields for the number of time intervals between the child observation and the potential parent observation, starting at the grid centroid closest to the child observation. At each time interval, the source probabilities for the location are calculated based on the vector fields and a gaussian representation of uncertainty (we used σ=5000 as a compromise between the standard deviations within our observed vector field (σ_{vx} = 3392 m, σ_{vy} = 8662 m)) and accumulated over the number of timesteps before being normalised in 0-1. The result is a probability field describing likelihoods for the source location of the child iceberg at a given lead time (inset panels to Figure A1). If a potential parent is located such that its associated probability of being a source is above a given, tuned, threshold of 0.05 (e.g it falls within the contour in Figure A1) it is included in the list of potential parents for that child iceberg.

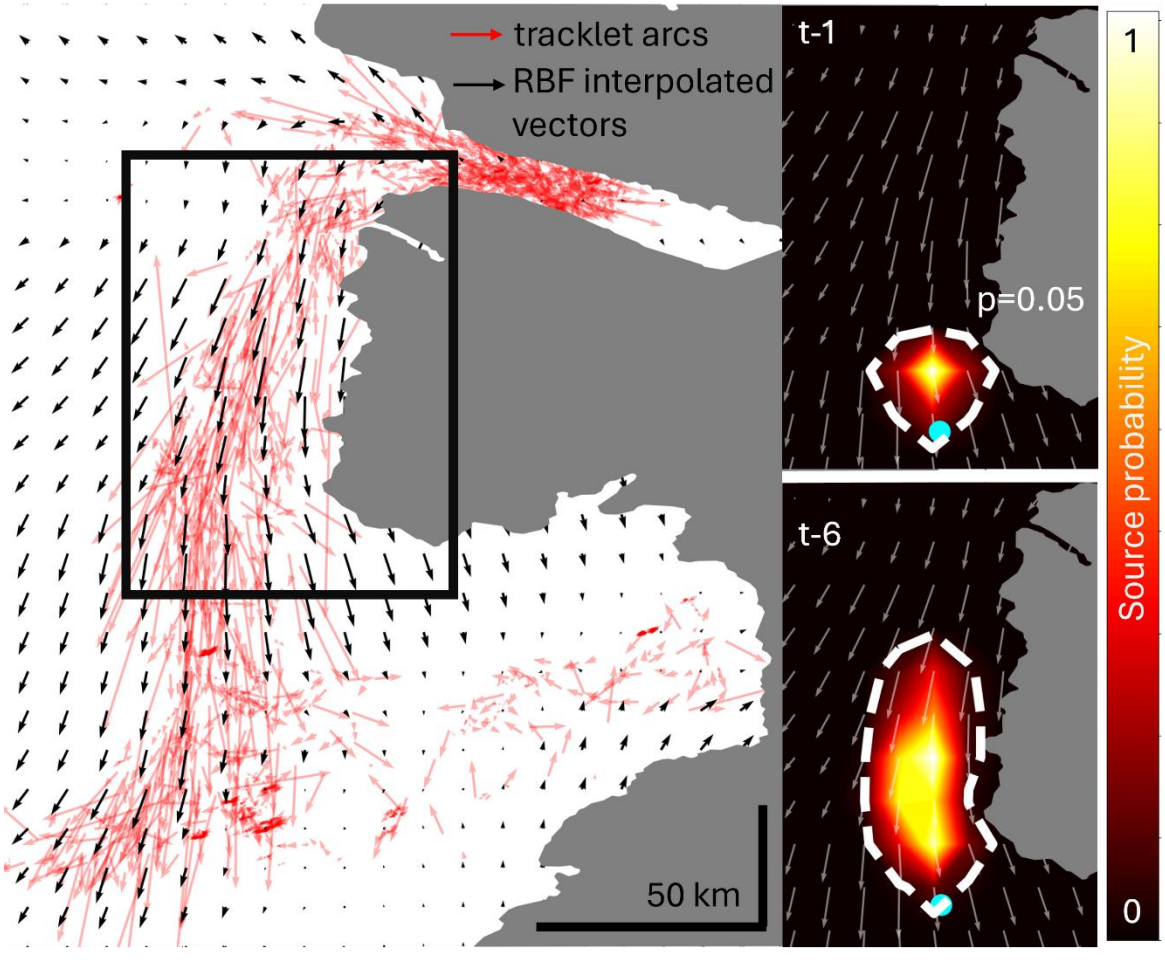

Figure A1 - temporally-densified tracklet arcs (red arrows) and radial basis function interpolated vector field (black arrows). Insets show illustrative probabilistic source map for example location of cyan dot within sub-region (black box) for lead times of 1 (top tight) and 6 (bottom right), with p=0.05 contour shown.

https://doi.org/10.5194/egusphere-2025-2886
Preprint. Discussion started: 7 July 2025

Appendix B: Exclusion of fjord

We tested the performance of generational linking in locations outside the fjord of Petermann Glacier. Within the fjord there is a propensity of the method to allocate newly-appearing icebergs to fragmentation of existing icebergs when in reality they are calving from the glacier tongue. As outlined in the discussion, this arises because out dataset does not include digitisations of the shape of the calving front itself so the tessellation process cannot allocate new tracklets to it as a source. Where the process finds a potential generational linkage, therefore, it allocates it without comparing with any geometric fit to the calving front.

To assess the impact of this limitation on the performance of our generational linking we evaluated our tracks against a subset of the dataset that excludes the fjord. Figure B1 shows the fjord area with only those icebergs calved in 2008 shown for clarity. All iceberg outlines that intersected with an area representing the fjord (hatched on Figure B1) were excluded from the dataset. The orange filled iceberg re-entered the fjord after being observed in this location and subsequently fragmented, with its children first being observed outside the fjord. The ID of this iceberg was manually updated to that of its last observed instance within the fjord prior to fragmentation to allow for correct assessment of the lineage of its children. The remainder of the tracking and evaluation procedure was unchanged.

https://doi.org/10.5194/egusphere-2025-2886
Preprint. Discussion started: 7 July 2025

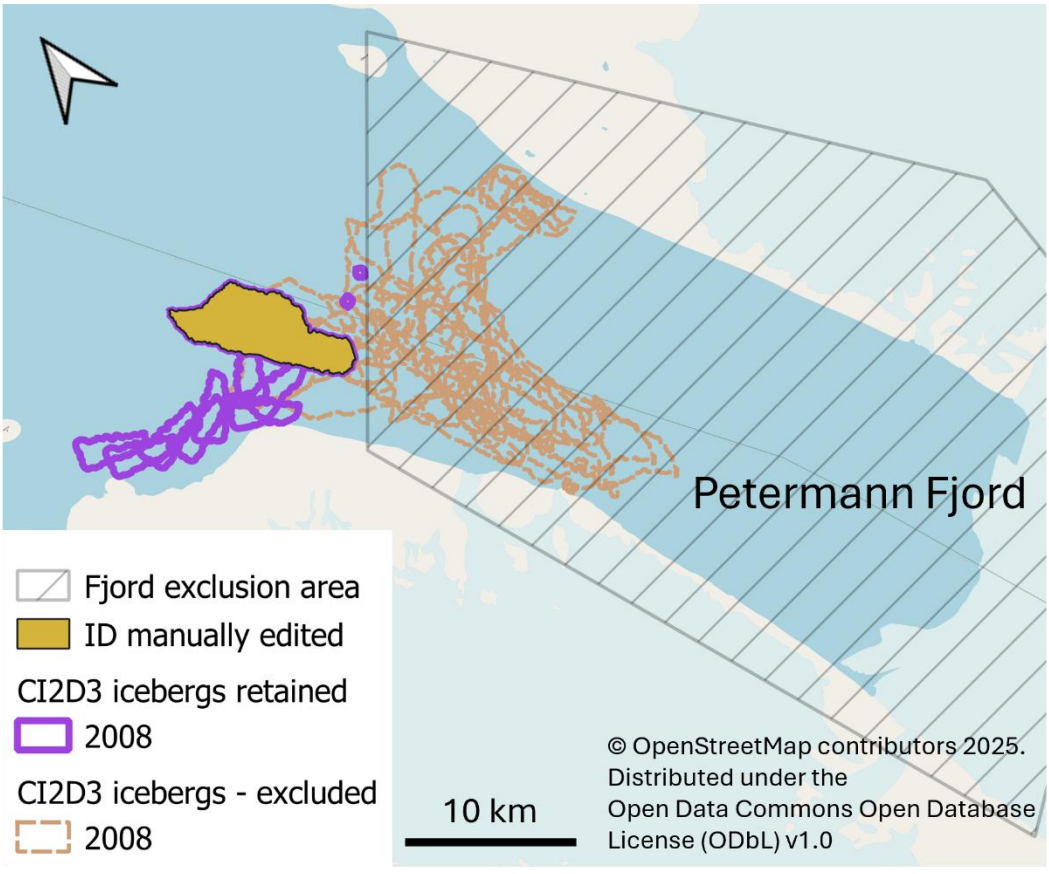

Figure B1 - Exclusion of icebergs within Petermann Fjord, showing only 2008 icebergs for clarity. Those intersecting with hatched fjord area were removed from dataset. The filled iceberg re-entered the hatched area before fragmenting so its ID was updated manually to allow correct evaluation of the lineage of the fragments. Map data: https://www.openstreetmap.org/copyright.

660